Eurocode Structural Fire Design and its Application for Composite Circular Hollow Section Columns

José Carlos L. Ribeiro
engjcarlos@yahoo.com.br
Federal University of Minas Gerais - UFMG
Structural Engineering Department
30310-060 Belo Horizonte, MG, Brazil

Ricardo H. Fakury
fakury@dees.ufmg.br

Estevam B. de Las Casas
Emeritus Member, ABCM
estevam@dees.ufmg.br

The tabular structural fire design method for centrally loaded composite columns consisting of concrete filled steel circular hollow sections proposed in EN 1994-1-2:2005 (Eurocode 4: Design of Composite Steel and Concrete Structures – Structural Fire Design) is described here. A design procedure is then discussed, based on the determination of the temperature distribution in the cross sectional area and along the column length. A finite element based computer program is developed to implement the three-dimensional thermal analysis of different materials and geometries for given time versus temperature fire data. An example problem is shown, comparing the tabular method proposed in EN 1994-1-2:2005 and the method presented in this work.
Keywords*: composite structures, concrete filled steel circular hollow columns, three-dimensional thermal analysis, finite element analysis, structural fire design*

Introduction

The alternatives proposed in EN 1994-1-2:2005 for the structural fire design of composite steel and concrete columns consist in three different levels of assessment: methods that include the use of tabular data (level 1), simple calculation models (level 2) and general calculation models (level 3).

The use of the simple calculation models recommended in EN 1994-1-2:2005 – chapter 4.3 requires the determination of the temperature distribution in the column's cross-section (temperature is taken as constant along the length). As this calculation involves either laboratory testing or the use of specific computer codes, the use of tabular data is more common, as it readily provides the standard fire resistance for a composite column given basic design information such as geometry, reinforcement and loading.

In this work, the tabular data design method described in EN 1994-1-2:2005 – chapter 4.2 for the case of centrally loaded concrete filled steel circular hollow sections is reviewed. A simple calculation model (level 2) based in EN 1994-1-2:2005 – chapter 4.3 is presented, but considering the temperature variation in the cross section and also along the length of the column. A description of an implementation of the solution model using finite elements as basis is also done, allowing the determination of the temperature distribution for different materials and geometry arrangements. An application example is then shown, with the detailed calculation for R30, R60, R90 and R120 of standard temperature-time curve as given by ISO 834-1:1999. For the example, both design methods are used, and a comparative analysis is performed, covering aspects such as safety and costs.

Nomenclature

a = vector of nodal temperatures
A_a = steel tube section area, cm²
A_c = concrete section area, cm²
A_s = steel reinforcement bars section area, cm²
B = matrix of heat flow x temperature relation
c = specific heat, J/(kg.K)
D = constitutive matrix resulting from the thermal conductivities λ
d = external diameter of the circular hollow section, cm
$d\theta/dn$ = temperature gradient, K/m
E_a = Young's modulus of the structural steel, kN/cm²
$E_{c,sec,\theta}$ = secant elastic modulus of the normal density concrete with temperature, kN/cm²
$(EI)_{fi,eff}$ = effective flexural stiffness in fire situation, kN.cm²
E_s = Young's modulus of the reinforcement steel, kN/cm²
f = nodal heat flow vector
f_{ay} = yield strength of the structural steel, kN/cm²
f_{ck} = compressive strength of the normal density concrete, kN/cm²
f_{sy} = yield strength of the reinforcement steel, kN/cm²
I_a = moment of inertia of the tubular steel section, cm^4
I_c = moments of inertia of the concrete elements, cm^4
I_s = moments of inertia of the reinforcement bars, cm^4
K = stiffness matrix
$k_{c,\theta}$ = reduction factor of compressive strength f_{ck} with temperature
$k_{E,\theta}$ = reduction factor of Young's modulus E_a with temperature
$k_{y,\theta}$ = reduction factor for yield strength f_{ya} with temperature
M = mass matrix
n = boundary's normal vector, given by its components n_x, n_y and n_z
N = matrix of functions of shape for the Finite Element Method
$N_{fi,cr}$ = elastic critical load under fire, kN
$N_{fi,d,t}$ = design load axial compressive resistance in fire situation, kN
$N_{fi,pl,Rd}$ = design value of the plastic resistance to axial compression in fire situation, kN
$N_{fi,Rd}$ = design value of the resistance in axial compression under fire, kN
N_{Rd} = design load axial compressive resistance for normal temperature, kN
q = heat flow per unit area, W/m²
$\bar{q}$ = prescribed heat flow per unit area, W/m²
t = time of assessment after fire's ignition, minutes
t_c = slab thickness, cm
u_s = distance between the reinforcements and internal surface of the steel tube, mm
W = arbitrary weighting functions to the Weighted Residuals Method

Greek Symbols

α = convection-radiation coefficient, W/(m².ºC)
α_c = convection coefficient, W/(m².K)
β = coefficient for the integration scheme
Γ_q = boundary with prescribed heat flow
Γ_θ = boundary with fixed temperature

Paper accepted December 2007. Technical Editor: Nestor A. Zouain Pereira.

Δt = time interval used by Finite Element Method to integrate the transient problem, seconds
$\varepsilon_{cu,\theta}$ = strain used to calculate the secant elastic modulus $E_{c,sec,\theta}$
ε_{res} = resultant emissivity for the surface
$\eta_{fi,t}$ = loading level at time t
θ = temperature at the surface of the body, K
$\overline{\theta}$ = fixed temperature at part of the boundary, K
θ_f = temperature for the fluid (heated gases), K
λ = thermal conductivity, W/(m.K)
$\overline{\lambda}_\theta$ = non-dimensional slenderness ratio
ρ = material density, kg/m³
ρ_i = heat density due to an internal source, W/m³
σ = Stefan-Boltzmann constant, taken as 5.6697x10^{-8} W/(m^2.K^4)
χ = reduction coefficient for buckling curve
Ω = domain of analysis
∇ = gradient operator, taken as $\partial/\partial x_i$, where x_i is the Cartesian coordinate system

Variation of Mechanical Properties with Temperature

In this item, the variation of the relevant material properties with temperature is described. Data are given for rolled structural steel and normal density concrete, as required for the application problem to be presented.

The reduction in the yield strength (f_{ay}) and Young's modulus (E_a) with temperature for rolled steel shapes is represented by factors $k_{y,\theta}$ and $k_{E,\theta}$, respectively, as shown in Table 1.

Table 1. Parameters for concrete and steel with temperature.

Temperature (ºC)	Steel		Concrete	
	$k_{y,\theta}$	$k_{E,\theta}$	$k_{c,\theta}$	$\varepsilon_{cu,\theta} \times 10^3$
20	1.000	1.0000	1.00	2.5
100	1.000	1.0000	1.00	4.0
200	1.000	0.9000	0.95	5.5
300	1.000	0.8000	0.85	7.0
400	1.000	0.7000	0.75	10.0
500	0.780	0.6000	0.60	15.0
600	0.470	0.3100	0.45	25.0
700	0.230	0.1300	0.30	25.0
800	0.110	0.0900	0.15	25.0
900	0.060	0.0675	0.08	25.0
1000	0.040	0.0450	0.04	25.0
1100	0.020	0.0225	0.01	25.0
1200	0.000	0.0000	0.00	–

The reduction factor $k_{c,\theta}$, to be applied to the compressive strength (f_{ck}) for normal density concrete is shown in Table 1. This table also depicts $\varepsilon_{cu,\theta}$ strain, used for the determination of the secant elastic modulus of concrete under high temperature as given in Eq. (1):

$$E_{c,\sec,\theta} = \frac{k_{c,\theta} f_{ck}}{\varepsilon_{cu,\theta}} \quad (1)$$

Design Using Tabular Data

The tabular data provided for the fire design of composite columns made of concrete filled steel hollow sections subjected to axial compressive loading are given in Table 2. In this table, the standard fire resistance is found as a function of the loading level $\eta_{fi,t}$, the external diameter d, the reinforcement rate, i.e., the ratio between the cross-sectional area of reinforcement and the total area, $A_s/(A_c+A_s)$, and the distance between the reinforcements and internal surface of the steel tube. Its use is restricted to the cases where the column's length is limited to 30 times the external diameter of the cross-section, the column is part of a braced frame and the fire is constrained to only one storey of the building, where the temperature is taken as uniform along the column length. Another hypothesis is that the reinforcement bars are rolled, with yield strength at room temperature of 500 MPa. The load level at time t, $\eta_{fi,t}$, is given by:

$$\eta_{fi,t} = \frac{N_{fi,d,t}}{N_{Rd}} \quad (2)$$

where $N_{fi,d,t}$ is the design load axial compressive resistance in the fire situation and N_{Rd} the design load axial compressive resistance for normal temperature.

The design load axial compressive resistance in the fire situation, $N_{fi,d,t}$, is determined combining the characteristic actions, as described in EN 1991-1-1:2002. Its value is usually smaller than 70% of the acting load for normal temperature design, taking into account the fact that fire is an exceptional event, with low probability of occurrence and short in duration, allowing for the use of smaller weighting coefficients for the characteristic actions than used for normal temperature design.

Table 2. Tabular data for fire design.

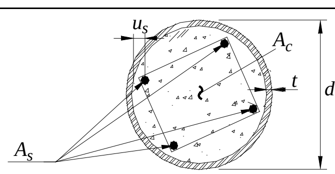		Standard fire resistance			
		R30	R60	R90	R120
1	*Minimum values for load level $\eta_{fi,t} \le 0.28$*				
	Diameter d (mm)	160	200	220	260
	Reinforcement rate $A_s/(A_c + A_s)$ in %	0	1.5	3.0	6.0
	Axis distance of reinforcement bars u_s (mm)	-	30	40	50
2	*Minimum values for load level $\eta_{fi,t} \le 0.47$*				
	Diameter d (mm)	260	260	400	450
	Reinforcement rate $A_s/(A_c + A_s)$ in %	0	3.0	6.0	6.0
	Axis distance of reinforcement bars u_s (mm)	-	30	40	50
3	*Minimum values for load level $\eta_{fi,t} \le 0.66$*				
	Diameter d (mm)	260	450	550	-
	Reinforcement rate $A_s/(A_c + A_s)$ in %	3.0	6.0	6.0	-
	Axis distance of reinforcement bars u_s (mm)	25	30	40	-

The design load axial compressive resistance for normal temperature, N_{Rd}, is obtained as proposed in EN 1994-1-1:2004. Nevertheless, the following considerations must be followed for the use of Eq. (2) (and only for this purpose):

- the buckling length for the column should be taken as twice the column length under fire;
- an upper bound of 235 MPa for yield stress should be assumed, regardless of the mechanical properties of the steel used for the tubular steel profile;
- the thickness of the steel circular tube cannot be taken as larger than 1/25 of its diameter;
- the reinforcement rate should be considered as less or equal to 3%.

Simplified Design Method

The simple calculation model for the design of composite columns under fire according to EN 1994-1-2:2005 – chapter 4.3 is based on a sound formulation, derived from classical principles of material science and structural analysis, and can be used for braced frames. It requires the determination of the temperature distribution in the cross sectional area of the column, considered to be constant along its length.

A simplified method is described in the following items, centered in the basic assumptions of EN 1994-1-2:2005 – chapter 4.3 and taking into account the work of Lawson and Newman (1996), but including the consideration of the temperature variation along the column length. In this manner, it is possible to consider the fact that temperatures in the fire compartment varies from a minimum close to the column ends (where connections, beams and concrete slabs are found) to a maximum at locations in the central portion of the column.

Next, the steps to be followed in the proposed simplified method are described:

a) Design Value of the Plastic Resistance to Axial Compression

The determination of the design value of the plastic resistance to axial compression under fire for composite columns can be performed for the section under higher temperature, in the central portion of the column, as:

$$N_{fi,pl,Rd} = A_a k_{y,\theta} f_{ay} + \sum_k \left(A_s k_{y,\theta} f_{sy}\right) + \sum_m \left(A_c k_{c,\theta} f_{ck}\right) \tag{3}$$

where the first term at the right side of the equation represents, at elevated temperature, the product of the steel tube section area by its yield point, the second term the sum of products of steel reinforcement bars section area by yield point and the third term the sum of products of concrete area by compressive strength of this material. In Eq. (3), the partial material safety factors were not shown, because they are equal to 1.00.

The temperature for the steel tube is taken as constant, due to its small thickness and the high thermal conductivity of steel. For each reinforcement bar, the temperature is function of its position and also taken as constant, due to their small diameters and high thermal conductivity. For concrete, temperature increases with radial distance from the center, as shown in Fig. 1.

b) Effective Flexural Stiffness

The effective flexural stiffness for the composite column is given by:

$$(EI)_{fi,eff} = k_{E,\theta} E_a I_a + \sum_k \left(k_{E,\theta} E_s I_s\right) + \sum_m \left(E_{c,\sec,\theta} I_c\right) \tag{4}$$

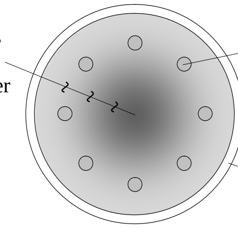

Figure 1. Temperature distribution for thecross section of composite column.

where the first term on the right side of the equation corresponds, at elevated temperature, to the moment of inertia of the tubular steel section times its Young's modulus, the second term the sum of the products of the moments of inertia of the reinforcement bars by their Young's modulus and the last term the sum of the products of the moments of inertia of the concrete elements by the secant Young's modulus for this material, according to Eq. (1).

The effective flexural stiffness varies along the column length, proportionally to temperature, as expected.

c) Elastic Critical Load

The elastic critical load under fire, $N_{fi,cr}$, should be calculated taking into account the variation of effective flexural stiffness along the length, as described in step **b** of the method. The load value depends on the buckling length under fire, usually determined as for normal temperature design. For multiple storey frames, the columns can be assumed as fixed in the fire compartments above and below, provided that the fire resistance of the buildings components that separate these fire compartments is not less than the fire resistance of the column.

The elastic critical load can be obtained using finite element computer programs based on the stability theory, including the consideration of stiffness degeneration due to normal compressive load and the second order effects in structural model. In this paper, the commercial program ANSYS (2004) was used to provide an eigenvalue-based solution for buckling analysis.

d) Non-Dimensional Slenderness Ratio

The non-dimensional slenderness ratio for the column under fire is given by Eq. (5):

$$\bar{\lambda}_\theta = \left(\frac{N_{fi,pl,Rd}}{N_{fi,cr}}\right)^{0,5} \tag{5}$$

where the values of $N_{fi,pl,Rd}$ and $N_{fi,cr}$ are obtained at steps **a** and **c**, respectively.

e) Design Value of the Resistance in Axial Compression

The design value in the fire situation of the composite column resistance in axial compression shall be obtained from:

$$N_{fi,Rd} = \chi \, N_{fi,pl,Rd} \tag{6}$$

where χ is the reduction coefficient for buckling curve *c* of EN 1993-1-1:2005, which depends on the non-dimensional slenderness ratio (see step **d**), and $N_{fi,pl,Rd}$ is obtained at step **a**.

It should be noticed that design value of resistance obtained herein, $N_{fi,Rd}$, considers the partial material safety factors equal to 1.00, as shown at step **a**.

Finite Element Calculation of Temperature Distribution

Heat Transfer Mechanisms

The standard formulation for the heat transfer problem is used in the numerical treatment of the problem (Huang and Usmani, 1994). Conduction is assumed to be represented by Fourier's law:

$$q = -\lambda \frac{d\theta}{dn} \tag{7}$$

where q is the heat flow per unit area, λ the thermal conductivity and $d\theta/dn$ the temperature gradient.

Convection is modeled by Newton's law:

$$q = \alpha_c \left(\theta - \theta_f\right) \tag{8}$$

where q is the heat flow per unit area, α_c the convection coefficient, θ the temperature at the surface of the body and θ_f the temperature for the fluid.

Radiation is assumed to follow Stefan-Boltzmann law:

$$q = \varepsilon_{res}\ \sigma \left(\theta^4 - {\theta_f}^4\right) \tag{9}$$

where q is the heat flow per unit area, ε_{res} the resultant emissivity for the surface, σ the Stefan-Boltzmann constant, θ the temperature at the body's surface and θ_f the average fluid temperature.

For the fire case, convection occurs between the heated gases and the surface of the structure. The determination of the fluid velocity due to convective flow is not required, and both radiation and convection at the boundary can be considered using a single boundary condition.

Finite Element Formulation

The heat transfer is assumed to follow the heat conduction basic equation, as given in Eq. (10):

$$\rho c \frac{\partial \theta}{\partial t} = \nabla^2 \mathbf{D} \theta + \rho_i \quad \text{in } \Omega \tag{10}$$

where θ is the temperature, t the time, ρ the material density, c the specific heat, ρ_i the heat density due to an internal source and **D** the constitutive matrix, resulting from the thermal conductivities λ, for the different dimensions of the domain Ω. For a three dimensional domain, **D** is given by:

$$\mathbf{D} = \begin{bmatrix} \lambda_x & 0 & 0 \\ 0 & \lambda_y & 0 \\ 0 & 0 & \lambda_z \end{bmatrix} \tag{11}$$

Boundary conditions for the problem can be either of the Dirichlet type, as given in Eq. (12), or Neumann's, as given in Eq. (13).

$$\theta - \overline{\theta} = 0 \quad \text{in } \Gamma_\theta \text{ (prescribed temperatures)} \tag{12}$$

$$-\mathbf{n}\, q + \alpha\left(\theta - \theta_f\right) + \overline{q} = 0 \quad \text{in } \Gamma_q \text{ (heat flows)} \tag{13}$$

For Eqs. (12) and (13), $\overline{\theta}$ is the fixed temperature value at part of the boundary, α represents the convection-radiation coefficient, $\overline{q}$ is the prescribed heat flow per unit area, θ_f the temperature of gases outside the domain, **n** the normal vector, given by:

$$\mathbf{n} = \begin{bmatrix} n_x & n_y & n_z \end{bmatrix}^T \tag{14}$$

The coefficient α covers both convection and radiation heat transfers, and is taken as:

$$\begin{aligned} \alpha = \alpha_c + \varepsilon_{res}\, \sigma \Big(& 4\times 273^3 + 6\times 273^2 \left(\theta_f + \theta\right) + \\ &+ \left(\theta_f + \theta\right)\left({\theta_f}^2 + \theta^2\right) + 4\times 273 \left({\theta_f}^2 + \theta_f\ \theta + \theta^2\right)\Big) \end{aligned} \tag{15}$$

where α_c is the convection coefficient, ε_{res} the resultant emissivity between gases and the surfaces, σ is the Stefan-Boltzmann constant ($5.669\text{x}10^{-8}$ W/m^2.K^4) and θ_f and θ are the temperatures, in degrees Celsius, for the gases and the surface. According to EN 1994-1-2:2005, α_c and ε_{res} can be taken as 25.0 W/(m².°C) and 0.50, respectively.

The integral form obtained using weighted residuals on Eq. (10) and the boundary conditions are given by Eq. (16). The arbitrary weighting functions are denoted by **W**. Neumann's boundary condition is included in the formulation, while the term due to Dirichlet boundary condition is automatically cancelled.

$$\begin{aligned} &\int_\Omega \mathbf{W}^T \left[\nabla^T \mathbf{D} \nabla \theta + \rho_i\right] \partial\Omega - \int_\Omega \mathbf{W}^T \rho c \frac{\partial \theta}{\partial t} \partial\Omega + \\ &\quad + \oint_{\Gamma_q} \overline{\mathbf{W}}^T \left[\mathbf{D} \nabla \theta + \alpha\left(\theta - \theta_f\right) + \overline{q}\right] \partial\Gamma_q = 0 \end{aligned} \tag{16}$$

Applying Green's theorem to the term $\nabla^T \mathbf{D} \nabla \theta$, ignoring the terms in the boundary with imposed temperatures and applying the Finite Element concepts, it can be shown that the matrix form of Eq. (16) is given by:

$$\mathbf{M} \frac{\partial \mathbf{a}}{\partial t} + \mathbf{K}\mathbf{a} = \mathbf{f} \tag{17}$$

In Eq. (17), **a** is the global vector containing the nodal temperatures, while **M**, **K** and **f** are the mass matrix, stiffness matrix and nodal heat flow vector, respectively. For each element, these matrices are given by Eqs. (18) to (20):

$$\mathbf{M}^{(e)} = \int_{\Omega^{(e)}} \rho c \mathbf{N}^T \mathbf{N}\, \partial\Omega^{(e)} \tag{18}$$

$$\mathbf{K}^{(e)} = \int_{\Omega^{(e)}} \mathbf{B}^T \mathbf{D} \mathbf{B}\, \partial\Omega^{(e)} + \alpha \oint_{\Gamma_q^{(e)}} \mathbf{N}^T \mathbf{N}\, \partial\Gamma_q^{(e)} \tag{19}$$

$$\mathbf{f}^{(e)} = \int_{\Omega^{(e)}} \mathbf{N}^T \rho_i\, \partial\Omega^{(e)} - \oint_{\Gamma_q^{(e)}} \mathbf{N}^T \overline{q}\, \partial\Gamma_q^{(e)} + \alpha \oint_{\Gamma_q^{(e)}} \mathbf{N}^T \theta_f\, \partial\Gamma_q^{(e)} \tag{20}$$

The transient solution is obtained by integration in time of Eq. (17). In this work, two assumptions were used to obtain the approximate discrete solution: first, Eq. (17) is satisfied only at time $t_{n+\beta}$ in each time interval Δt, and second, temperatures vary linearly within each time interval.

Using these concepts in Eq. (17), the recurrence Eq. (21) is obtained:

$$\left[\frac{\mathbf{M}_{n+\beta}}{\beta\,\Delta t}+\mathbf{K}_{n+\beta}\right]\mathbf{a}_{n+\beta}=\mathbf{f}_{n+\beta}+\frac{\mathbf{M}_{n+\beta}}{\beta\,\Delta t}\,\mathbf{a}_n \qquad (21)$$

Matrices $\mathbf{M}_{n+\beta}$, $\mathbf{K}_{n+\beta}$ and $\mathbf{f}_{n+\beta}$ are calculated for $t_{n+\beta}$. After solving the system in Eq. (21) for $\mathbf{a}_{n+\beta}$, temperatures at the end of the interval Δt are given by:

$$\mathbf{a}_{n+1}=\frac{1}{\beta}\,\mathbf{a}_{n+\beta}+\left(1-\frac{1}{\beta}\right)\mathbf{a}_n \qquad (22)$$

where $\mathbf{a}_n$ are the initial temperatures for the next time step.

The trapezoidal time integration rule in Eq. (21) is conditionally stable (Hogge, 1981), converging for $0.5 \le \beta \le 1$. The solution becomes more stable as β approaches unity (Backward Euler). At that point, there are no more oscillations, and the obtained solution is normally underestimated. Vila Real (1988) suggested the use of the Galerkin scheme, with $\beta = 2/3$, and shows that this choice results in faster convergence to the exact solution.

Computer Program Description

A finite element program for thermal analysis based on the theoretical developments described before was developed and named *Thersys*, based on the *Caltemi* platform, according to Fakury et al. (2002) and on program *Caltep*, from CIMNE (1993) in Barcelona. Program *Thersys* allows the use of different fire curves, modeling of solid structures and the consideration of non-linear thermal material properties. The assumed values for thermal conductivity, specific heat and mass density for steel and concrete were taken from EN 1994-1-2:2005.

The program includes the following isoparametric elements:

• 3 node triangular Lagrangian and 6 node serendipity triangle, 4 and 9 node quadrangular Lagrangian and 8 node serendipity quadrangular elements;

• 4 node Lagrangian tetrahedral and 10 node serendipity tetrahedral, 8 node Lagrangian and 20 node serendipity hexahedra.

Four different boundary conditions can be considered in the program:

• prescribed temperature, or Dirichlet condition;

• prescribed heat flow, or Neumann condition;

• cooling condition in the boundary, given by:

$$-\lambda\frac{\partial\theta}{\partial n}=\alpha_c(\theta-\theta_f)+\varepsilon_{res}\sigma(\theta^4-\theta_f^4) \qquad (23)$$

where α_c is the natural convection coefficient between the outside environment and the structure, ε_{res} the resultant emissivity between the surface and external media, which is taken as 0.5, σ is Stefan-Boltzmann's constant, taken as $5.669\text{x}10^{-8}$ W/m^2.K^4 and θ_f the normal temperature, normally assumed to be 20 ºC;

• fire condition, also represented by Eq. (23), now with α_c as the forced convection coefficient between the environment and the structure surface and θ_f as the external temperature, variable according to a defined curve.

The convection coefficients are taken as 12.834 W/m².ºC, 3.145 W/m².ºC, 9.909 W/m².ºC and 25.000 W/m².ºC, respectively, for cooling condition in hot surface with that surface turned up, cooling condition in hot surface turned down, cooling condition with hot surface in the vertical position and fire condition (Ribeiro, 2004).

Example

Problem Description

The analysis of a composite column made of a steel circular tube filled with reinforced concrete is described in this item. The tube, shown in Fig. 2, is 5.6 mm thick and 355.6 mm in diameter, with yield strength (f_{ay}) of 235 MPa. The concrete has compressive strength (f_{ck}) of 30 MPa and moisture content varying among 0%, 4% and 10% of concrete weight. The reinforcement consists of eight 22 mm steel bars with yield strength (f_{sy}) of 400 MPa. The column is assumed to be in a multiple storey building with 4 m between floors. The concrete slabs have constant thickness of 120 mm.

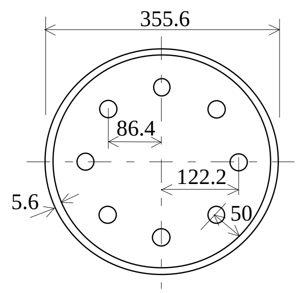

Figure 2. Composite column cross-section (dimensions in millimeters).

Temperature in the Column Using Finite Element Analysis

The temperature distribution in different sections of the column was calculated using Finite Element Analysis. Sections 1 to 6, shown in Fig.3-a, were considered for R30, R60, R90 and R120 of standard temperature-time curve as given by ISO 834-1:1999, including the influence of the slabs in the ends of the column.

Section 1 was located at the concrete slab mid-section (considered as the extremity of the column); section 2 in the lower surface of the slab, section 3 to 5 at intervals of t_c / 2 from each other, down from section 2, section 6 at the column centre (t_c is the slab thickness).

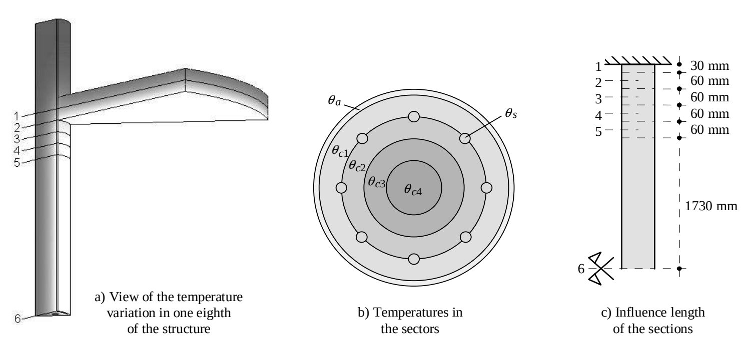

Figure 3. Geometric description of the model and relevant cross-sections.

The obtained temperature distribution was almost symmetrical to the column central section (section 6), and that result was used in the design. For each section, the concrete area was divided in four concentric circular sectors of equal thickness, as shown in Fig.3-b.

The mean values between the obtained temperatures in the area of each sector are shown in Table 3 for concrete with 4% of moisture content.

As there are four planes of symmetry, only one eighth of the geometry was modeled (Fig.3-a), using a mesh with 60156 nodes and 313634 four node tetrahedral Lagrangian elements. The mesh density was shown to be appropriate to obtain convergence to the finite element solution (Ribeiro, 2004).

Comparison Between the Tabular Data and the Presented Simplified Method

a) Design Load Compressive Resistance for Normal Design

In order to find the design load axial compressive resistance in fire situation using the tabular data, $N_{fi,d,t}$, firstly the load level $\eta_{fi,t}$ has to be calculated, as a function of the load compressive resistance for normal design, N_{Rd}, as discussed before. N_{Rd} was calculated for a buckling length of 4 m (twice the buckling length under fire – seen before) with the yield strength for the steel of the tube as 235 MPa. Noting that for the column the tube thickness is less than 1/25 of its diameter and that the reinforcement rate does not reach 3%, a value of N_{Rd} equal to 3622 kN was found.

b) Design Load Compressive Resistance in Fire Situation

Based on the temperature values, the results for the column are listed in 12 segments (6 at each side of the central cross section) of different effective stiffness values (the values of temperatures and effective stiffness are shown in Table 3). The elastic buckling load, discussed in item **c** of topic "*Simplified Design Method*", was obtained taking the temperature obtained for section 1 for the upper 30 mm of the column, temperatures for sections 2 to 5 in the next segments, each with a 60 mm length, and the temperature in section 6 for the next segment, with 1730 mm length, shown in Fig.3-c, as the region of significant temperature gradients is restricted to the column ends.

Table 4 presents the obtained results for design load compressive resistance in fire situation for the example problem using both methods, tabular and the simplified, presented in this work, according to the temperature distribution obtained from three-dimensional (3D) Finite Element Analysis.

Table 3. Temperatures and effective stiffness for concrete with 4% of humidity (see Fig. 3).

Standard Fire Resistance	Section	Temperature (ºC)						$(EI)_{fi,eff}$ (kN.cm²)
		Steel		Concrete				
		θ_a	θ_s	θ_{c1}	θ_{c2}	θ_{c3}	θ_{c4}	
R30	1	131	48	79	36	23	20	300488713
	2	388	74	178	55	27	21	234887882
	3	568	94	260	68	30	22	165722808
	4	612	102	281	72	31	22	141239020
	5	622	104	283	73	31	22	137504125
	6	624	105	286	73	31	22	136572215
R60	1	247	108	162	85	49	34	260970166
	2	590	168	348	126	66	42	139370143
	3	799	220	469	163	78	49	79600702
	4	840	245	501	179	83	52	74804937
	5	847	254	506	185	84	53	73609384
	6	848	258	510	187	84	54	73118385
R90	1	331	169	244	130	85	64	231364795
	2	708	259	460	211	108	81	83442951
	3	914	330	601	273	126	93	61264925
	4	941	367	635	299	136	98	57383783
	5	945	381	642	310	140	100	56110528
	6	946	389	646	314	142	101	55497035
R120	1	396	227	310	186	115	94	208904210
	2	790	334	544	288	154	111	67734530
	3	980	418	690	362	195	122	50699036
	4	1001	462	725	395	218	129	46613698
	5	1004	480	733	409	228	133	45169216
	6	1005	492	739	416	233	134	44346035

Table 4. Comparative results for design load compressive resistance.

Standard Fire Resistance	Simplified Method Presented - $N_{fi,Rd}$ (kN)						Tabular Data		Twilt
	Humidity of 0%		Humidity of 4%		Humidity of 10%		Maximum $\eta_{fi,t}$	$N_{fi,d,t}$ (kN)	$N_{fi,Rd}$ (kN)
	3D	2D	3D	2D	3D	2D			
R30	3881	3882	3996	3998	4151	4153	0.660	2390	-
R60	2976	2973	3074	3071	3189	3186	0.470	1702	2753
R90	2511	2511	2657	2656	2779	2778	0.280	1014	2261
R120	1967	1962	2176	2173	2402	2400	-	-	1840

In this table, it is also shown the design load compressive resistance in fire situation using the hypothesis adopted by EN 1994-1-2:2005 – chapter 4.3, which the temperature distribution in the cross section is constant along the length of the column. This case was calculated using the two-dimensional (2D) temperature distribution obtained at section 6 at the column centre.

Table 4 also presents the design load compressive resistance for the same column shown in Twilt et al. (1994). These results were obtained by a computer program developed and verified by Valexy (Twilt et al., 1994). This program was modified in order to reach compliance with more recent test results.

Comparing the results shown in Table 4, it can be noticed that the axial forces in the composite column in the example are significantly smaller when calculated from the tabular data, suggesting that it provides a considerably conservative approach.

Another interesting result is that the resistant axial forces are approximately 0.2% smaller than the results obtained for the simple calculation model (3D) if the analysis is performed assuming the temperature constant and equal to that of the central section of the column, that is, using a two-dimensional (2D) model for the temperature distribution, as proposed in EN 1994-1-2: 2005 – chapter 4.3. The small difference presented in Table 4 can be justified due to the reduced variation of temperature along the length for the proposed example.

If the real distribution of the temperatures external to the column (gases) is known along the column length, or in the case when temperature of the floors above and below the column are different, the plane model might no longer be realistic, while the use of the proposed method would provide a sound basis for the design.

The results also show that concrete humidity is an influent parameter in design load compressive resistance. On the other hand, it is a parameter difficult to obtain. In the example problem presented, for a fire of 120 minutes, an increase of approximately 22% in the design load compressive resistance is obtained comparing columns made with concrete with 0% and 10% of moisture content. According to EN 1994-1-2:2005, moisture content of 10% may occur for hollow sections filled with concrete.

Figure 4 presents graphically the results, including the value of the design load compressive resistance for room temperature, according to EN 1994-1-1:2004.

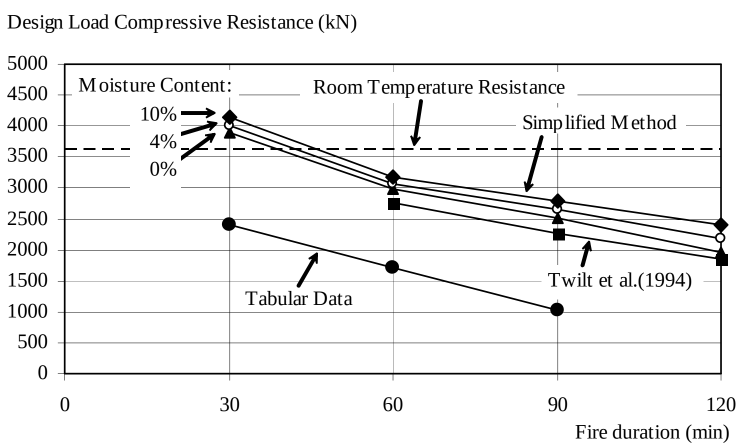

Figure 4. Comparative results for design load compressive resistance.

Final Remarks

In this paper a simplified method for the design of composite columns in fire situation was presented, consisting in taking into account the temperature variation in the column along the length as well as in the cross section. In order to implement the analysis, a model of a column under fire was described based on the heat transfer laws, as well as a three-dimensional finite element formulation and its implementation in a computer code. The program allows the analysis of either homogeneous or composite columns under fire.

The method was then used for the analysis of a composite column consisting of a steel tube filled with reinforced concrete submitted to axial load under fire. For the example, the results were compared to the design load obtained for the procedure given in based on tabular data, EN 1994-1-2: 2005 – chapter 4.2, resulting in considerable differences. These differences suggest that a more detailed analysis can, in this case, lead to lighter and cheaper structures. The results were also compared to the ones presented by Twilt et al. (1994), with good agreement. In the presented example, the moisture content of concrete was shown to be an important parameter, causing a 22% variation in the design load compressive resistance for a 120 minutes fire.

Finally, it is important to point out that the use of the presented design method depends on a more extensive comparison with laboratory test results, not yet available in scientific literature.

Acknowledgements

The authors acknowledge the support of the Brazilian funding agency CNPq (Conselho Nacional de Desenvolvimento Científico e Tecnológico) and CBCA (Centro Brasileiro da Construção em Aço).

References

ANSYS, 2004, “Finite Element Program – User’s Manual”, Version 9.0, ANSYS Inc., Canonsburg - USA.

European Committee for Standardization, 2002, “Actions on structures”. General actions. Eurocode 1 – EN 1991-1-1, Brussels, Holland.

European Committee for Standardization, 2004, “Design of composite steel and concrete structures”. General rules and rules for buildings (Part 1.1). Eurocode 4 – EN 1994-1-1, Brussels, Holland.

European Committee for Standardization, 2005, “Design of composite steel and concrete structures”. Structural fire design (Part 1.2). Eurocode 4 – EN 1994-1-2, Brussels, Holland.

European Committee for Standardization, 2005, “Design of steel structures”. General rules and rules for buildings (Part 1.1). Eurocode 3 – EN 1993-1-1, Brussels, Holland.

Fakury, R. H., Las Casas, E. B., Figueiredo Jr, F. P., Abreu, L. M. P., 2002, “Numerical analysis of Eurocode assumptions of temperature distribution of composite steel and concrete beams”. VII Mecon, Paraná, Argentina.

Hogge, M. A., 1981, “Comparison of two-level and three-level integration schemes for non-linear heat conduction”. In: Zienkiewicz, O. C.; Lewis, R. W.; Morgan, K. “Numerical Methods in Heat Transfer”. Bristol, John Wiley & Sons LTD, UK.

Huang, H., Usmani, A. S., 1994, “Finite element analysis for heat transfer”. Springer-Verlag London Ltd. Swansea, UK.

International Organization for Standardization, 1999, “Fire resistance tests - Elements of buildings construction” (Part 1). ISO 834-1, Geneva, Italy.

Lawson, R. M., Newman, G. M., 1996, “Structural fire design to EC3 & EC4, and comparison with BS 5950” – Technical Report, SCI Publication 159. The Steel Construction Institute, Silwood Park, UK.

Ribeiro, J. C. L., 2004, “Simulation by Finite Element Method of the three-dimensional temperature distribution in structures under fire” (In Portuguese). M. Sc. Thesis, School of Engineering, Federal University of Minas Gerais, Belo Horizonte, Brazil.

Twilt, L. Hass, R. Klingsch, W. Edwards, M. Dutta, D., 1994, “Design Guide for structural hollow section columns exposed to fire”. Construction with hollow steel sections, CIDECT. Verlag TÜV Rheinland, Germany.

Vila Real, P. J. M., 1988, “Finite Element modeling of the thermal and thermo elastic behavior of solids under high thermal gradients” (In Portuguese), M. Sc. Thesis, School of Engineering, University of Porto, Porto, Portugal.

Zárate, F. C., Onãte, E., 1993, “Caltep: Program for transient analysis of the Poisson’s Equation” (In Spanish). CIMNE publication number 27, Barcelona, Spain.